does He absorb significant internal energy in electronic excitations because its band gap is large compared with the temperature at relevant densities. Thus, He has a positive definite rate of increase of temperature with pressure, which most likely causes a positive total slope of temperature with pressure for the hydrogen-He mixture. In the metallic molecular fluid at 140 GPa and above, temperature variations have a weak effect on the electrical conductivity. In the semiconducting fluid at pressures P of 60 to 140 GPa, only a ~2% increase in temperature is sufficient to increase dT/dP from slightly negative for hydrogen (Fig. 2) to slightly positive for the hydrogen-He mixture. The latter is likely the case because Jupiter contains ~10 atomic % He. Temperature differences of a few percent have a negligible effect on the calculated conductivities (Fig. 3). Thus, the conductivities calculated here are consistent with a positive slope of dT/dP in Jupiter. To produce convection, dT/dP must be positive so that the volume coefficient of thermal expansion is also positive. Jupiter is known to be convective over most of its volume because it has a large external magnetic field. In addition, convective heat transfer to the surface is substantial and is the reason why Jupiter radiates more internal energy than it receives from the sun (*11*). It is possible, however, that Jupiter is convectively quiescent over a radially thin region (*6*).

REFERENCES AND NOTES

1. W. B. Hubbard, *Science* **214**, 145 (1981).
2. D. J. Stevenson, *Annu. Rev. Earth Planet. Sci.* **10**, 257 (1982).
3. V. N. Zharkov and V. P. Trubitsyn, in *Jupiter*, T. Gehrels, Ed. (Univ. of Arizona Press, Tucson, AZ, 1976), p. 145.
4. V. N. Zharkov and T. V. Gudkova, in *High-Pressure Research: Application to Earth and Planetary Sciences*, Y. Syono and M. H. Manghnani, Eds. (Terra Scientific Publishing, Tokyo, 1992), pp. 393–401.
5. M. Ross, H. C. Graboske, W. J. Nellis, *Philos. Trans. R. Soc. London Ser. A* **303**, 303 (1981).
6. W. J. Nellis, M. Ross, N. C. Holmes, *Science* **269**, 1249 (1995).
7. E. J. Smith, L. Davis, D. E. Jones, in *Jupiter*, T. Gehrels, Ed. (Univ. of Arizona Press, Tucson, AZ, 1976), p. 788.
8. W. B. Hubbard, *Planetary Interiors* (Van Nostrand-Reinhold, New York, 1984), p. 141.
9. D. J. Stevenson, *Rep. Prog. Phys.* **46**, 555 (1983).
10. ——— and E. E. Salpeter, *Astrophys. J. Suppl. Ser.* **35**, 221 (1977); D. J. Stevenson and N. W. Ashcroft, *Phys. Rev. A* **9**, 782 (1974).
11. W. B. Hubbard and M. Lampe, *Astrophys. J. Suppl. Ser.* **18**, 297 (1969); W. B. Hubbard, *Astrophys. J.* **152**, 745 (1968).
12. R. L. Kirk and D. J. Stevenson, *ibid.* **316**, 836 (1987).
13. R. Smoluchowski, *ibid.* **200**, L119 (1975).
14. R. Hide, *Nature* **280**, 42 (1979).
15. N. C. Holmes, M. Ross, W. J. Nellis, *Phys. Rev. B* **52**, 15835 (1995).
16. S. T. Weir, A. C. Mitchell, W. J. Nellis, *Phys. Rev. Lett.* **76**, 1860 (1996).
17. W. J. Nellis, A. C. Mitchell, P. C. McCandless, D. J. Erskine, S. T. Weir, *ibid.* **68**, 2937 (1992).
18. F. Hensel and P. P. Edwards, *Phys. World* **9**, 43 (1996).
19. N. W. Ashcroft, *Phys. Rev. Lett.* **21**, 1748 (1968).
20. N. F. Mott and E. A. Davis, *Electronic Processes in Non-Crystalline Materials* (Oxford, London, 1971), p. 81.
21. T. Guillot, D. Gautier, G. Chabrier, B. Mosser, *Icarus* **112**, 337 (1994).
22. T. Guillot, G. Chabrier, P. Morel, D. Gautier, *ibid.*, p. 354.
23. N. F. Mott, *Philos. Mag.* **24**, 2 (1971).
24. C. Freidli and N. W. Ashcroft, *Phys. Rev. B* **16**, 662 (1977).
25. B. I. Min, H. J. F. Jansen, A. J. Freeman, *ibid.* **33**, 6383 (1986).
26. D. Saumon, G. Chabrier, H. Van Horn, *Astrophys. J. Suppl. Ser.* **99**, 713 (1995).
27. D. M. Ceperley and B. J. Alder, *Phys. Rev. B* **36**, 2092 (1987).
28. N. W. Ashcroft, *ibid.* **41**, 10963 (1990).
29. W. J. Nellis *et al.*, *Science* **240**, 779 (1988).
30. A. A. Abrikosov, *Sov. Phys.-JETP* **18**, 1399 (1964).

31. This work was performed under the auspices of the U.S. Department of Energy by the Lawrence Livermore National Laboratory (LLNL) under contract W-7405-ENG-48 with support from the LLNL Directed Research and Development Program and NASA under grant W 16.180. We thank M. Ross and D. Saumon for providing isentropes of hydrogen; N. W. Ashcroft, W. B. Hubbard, D. J. Stevenson, and A. A. Abrikosov for helpful discussions; E. See, P. McCandless, J. Crawford, K. Stickle, W. Brocious, S. Weaver, J. Ulrech, and R. Silva for assistance in performing these experiments; and R. Kays of the Lockheed-Martin Company for providing the liquid hydrogen storage dewar.

13 February 1996; accepted 24 June 1996

Short-Period Comets: Primordial Bodies or Collisional Fragments?

Paolo Farinella* and Donald R. Davis

Modeling results show that collisions among Edgeworth-Kuiper Belt Objects (EKOs), a vast swarm of small bodies orbiting beyond Neptune, have been a major process affecting this population and its progeny, the short-period comets. Most EKOs larger than about 100 kilometers in diameter survive over the age of the solar system, but at smaller sizes collisional breakup is frequent, producing a cascade of fragments having a power law size-frequency distribution. Collisions are also a plausible mechanism for injecting EKOs 1 to 10 kilometers in diameter into dynamical resonances, where they can be transported into the inner solar system to become short-period comets. The fragmental nature of these comets may explain their physical properties, such as shape, color, and strength.

Comets were recognized as visitors from the outer periphery of the solar system almost half a century ago. Long-period ($P >$ 200 years) comets come from the nearly isotropic Oort cloud, tens of thousands of astronomical units (AU) from the Sun, whereas short-period comets may be derived from the transneptunian, flattened Edgeworth-Kuiper (E-K) Belt, at semimajor axes starting at about 35 AU and extending to 50 AU or beyond (*1*). These two different sources explain the different dynamical features of the two types of comets, in particular the much lower typical inclinations of the short-period group (*2*). Also, both types are plausible remnants of the accumulation of planetesimals in the outer regions of the primordial solar nebula (*3*). As a consequence, comets were considered to be the most primitive small bodies in the solar system: planetesimals from the giant planet zone that have never undergone the thermal and collisional processing that is typical of planets, satellites, and asteroids. This paradigm has been the basis for most recent studies on the structure of comet nuclei and their physical properties (*4*). However, we believe that the primitiveness paradigm is unwarranted for short-period comets derived from the transneptunian region, because significant collisional processing takes place there.

The discovery of the transneptunian object 1992 QB_1 and its successors (*5*) has confirmed the earlier theoretical evidence for a population of bodies beyond the giant planets. By early 1996, 32 objects had been discovered in this zone (besides the Pluto-Charon system). These objects are between 100 and 350 km in diameter, assuming a geometric albedo of 0.04. The total population of EKOs is estimated at (1 to 3) × 10^4, with diameters between ≈100 and 400 km at distances of 35 to 50 AU from the Sun, based on the total area searched to date. The distribution of eccentricities and inclinations is poorly known, but average values are probably low (≈0.05 for eccentricities and several degrees for inclinations) if the orbits are to be stable over the age of the solar system (*6*). An even more numerous population (at least ≈10^8 bodies) at diameters of about 20 km is probably present in the same zone, on the basis of results of recent Hubble Space Telescope

P. Farinella, Dipartimento di Matematica, Università di Pisa, Via Buonarroti 2, 56127 Pisa, Italy.
D. R. Davis, Planetary Science Institute, 620 North Sixth Avenue, Tucson, AZ 85705–8331, USA.

*To whom correspondence should be addressed.

(HST) searches (7). Finally, to provide the observed flux of short-period comets into the planet-crossing region, the population of EKOs about 2 km in diameter must be $\approx 5 \times 10^9$ (8).

Although these data constrain the EKO size distribution in an approximate way, they are enough to conclude that collision rates in the E-K Belt are not negligible, and we will argue as a consequence most kilometer-sized EKOs are probably collisional products. Collisions among EKOs have been shown (9) to occur frequently over the age of the solar system, a finding that is based on reasonable assumptions about the size and orbital distributions of EKOs and calculations of collisional probabilities. We have confirmed this result by another method. The collision rate within a population of orbiting objects depends on two factors: (i) the orbital distribution of the bodies and (ii) their number as a function of size. We applied a method for studying asteroid collisional rates and impact velocities developed by Wetherill (10). In this method, the orbital parameters allow one to derive for any pair of overlapping Keplerian orbits the so-called intrinsic collision probability P_i (which is zero for noninteracting orbits). For a population of orbiting bodies, the average intrinsic collision probability $<P_i>$ and impact velocity $<V>$ can be computed and used to estimate the prevailing collision rates (11). Our results for different sets of EKO orbits show that $<P_i>$ in the E-K Belt near 42 AU is $\approx 1.5 \times 10^{-21}$ km^{-2} year^{-1} (12), which is about 2000 times lower than the corresponding value for the asteroid belt (11). The asteroid belt contains only a few tens of bodies more than 200 km in diameter and probably a few million bodies more than 1 km, so the $\approx$1000 times larger EKO population approximately compensates for the lower $<P_i>$. Hence the frequency of impacts onto a target of any given size is roughly the same in the two populations. However, $<V>$ for the E-K Belt near 42 AU is ≈ 0.5 km s^{-1} (12), which is about a factor of 10 lower than for the asteroids (11).

We applied a numerical code developed to study the asteroid belt (13) to model the collisional evolution of EKOs. This code uses a series of diameter bins to represent populations of arbitrary size distributions and calculates the collisional interactions of each bin with every other one during a sequence of small time steps. These interactions are summed up at the end of each time step to give the net change in the population as a function of size; the updated population is used for the next time step. In this way, the time evolution of the population can be calculated. The orbital element distribution of the population was assumed to be unaltered by the collisions—a good approximation when the orbital energy due to random motions (that is, eccentricities and mutual inclinations) is large as compared with the collisional energy needed to significantly alter the population. The numerical code was modified to use values of $<P_i>$ and $<V>$ that were consistent with the results for EKO orbits.

Our current understanding of how cometary bodies would respond to collisions at speeds of hundreds of meters per second is limited. A critical parameter for our model was how much collisional energy is needed to fracture a body of a given size (dynamical strength). We assume that EKOs are rather weak bodies (as compared with most asteroids) in terms of their dynamic impact strength. It is important to note that dynamic impact strength provides a different measure of strength than tensile strength, which is believed to be small in comets because of observations of splitting events and the breakup of comet Shoemaker-Levy 9 from low tidal stresses during a jovian encounter. Impact experiments showed that specific energies on the order of a few times 10^6 erg g^{-1} were needed to shatter weakly bound aggregate bodies (14) or icy targets (15). We assumed an impact strength of 3×10^6 erg cm^{-3}, which is 10 times lower than the value adopted for asteroids and is appropriate for silicate targets.

Another assumption was that EKOs break up into a power-law size distribution of fragments moving relative to one another. The speed of the fragments is critical when the target has a gravity field—fragments moving slower than the local escape speed reaccumulate to form rubble pile structures. In our model, fragment speeds were controlled by the parameter f_{KE}, which specifies the fraction of collisional kinetic energy that goes into fragment kinetic energy and is estimated to be ≈ 0.1 from the properties of asteroid families (13).

In our baseline case (16), the initial EKO population was assumed to have a power-law distribution at diameters smaller than 300 km and included no object larger than 500 km. The orbital distribution corresponds to impact speeds between 350 and 550 m s^{-1}. After 4.5×10^9 years of collisional evolution, the population at diameters larger than 100 km was essentially unchanged (Fig. 1) because at the relatively low impact speeds found in this population, even a collision between equal-sized objects cannot break up bodies larger than about 100 to 150 km. However, at diameters smaller than 100 km, there was increasing collisional depletion with decreasing size; for diameters $\approx$20 km, the population was reduced from the initial one by a factor of 10. The slope of the small-sized population was close to -3.5, the equilibrium value for a collisionally relaxed population with size-independent collisional physics (17).

The -3.5 exponent provides only a marginal match to the few observational constraints on the abundance of EKOs. With such a power law, the abundance ratio between kilometer-sized comets and HST-discovered bodies with a radius of 10 km should be $\approx$300 (assuming equal logarithmic bins) instead of $\approx$30, as suggested from the available data. However, the HST data are consistent with a power-law exponent in the range -3 to -5 (18), which includes the equilibrium value. The available observations only provide an order-of-magnitude estimate of the real populations of EKOs, so it is premature to draw any conclusion about the collisional physics (for example, a possible size dependence of the impact strength or f_{KE}) from a comparison of the model results to observations.

The bodies surviving from the original population at diameters $D \approx 20$ km represented about 50% of the current population (Fig. 1). The survivor fraction increased with size, and for $D > 80$ km, essentially all of the bodies were survivors. Below $D \approx 20$ km, though, survivors were rare and at diameters of a few kilometers, virtually all bodies were collisionally derived fragments.

We varied the starting population to see how sensitive the results were to the initial conditions (12). A steeper initial population at small sizes (power-law exponent of -4) again showed depletion due to collisions starting at diameters of about 100 km, with a much stronger reduction in the number of bodies (by about a factor of 70) for

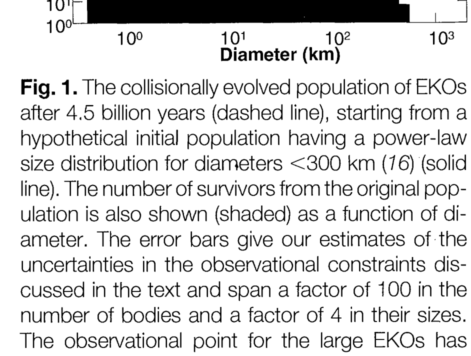

Fig. 1. The collisionally evolved population of EKOs after 4.5 billion years (dashed line), starting from a hypothetical initial population having a power-law size distribution for diameters <300 km (16) (solid line). The number of survivors from the original population is also shown (shaded) as a function of diameter. The error bars give our estimates of the uncertainties in the observational constraints discussed in the text and span a factor of 100 in the number of bodies and a factor of 4 in their sizes. The observational point for the large EKOs has smaller uncertainty in the population, reflecting a more reliable estimate of their numbers.

$D \approx 1$ km. Again, though, the slope of the small-sized end of the distribution was -3.5. On the other hand, a shallower starting slope (-3) yielded a lower depletion, only about 50% at $D \approx 30$ km, and actually gave a final population two times as large as the starting one at $D \approx 1$ km. Using starting populations close to the current one at $D > 300$ km and assuming power laws with different exponents for smaller sizes, we estimate that the initial small-size exponent had to be <-2, otherwise the current reservoir of short-period comets would be too small. Hence, at the end of the accretionary phase, there must have been a sizeable population of bodies down to at least a few tens of kilometers in diameter. However, all the smaller (kilometer-sized) bodies may well have been generated as fragments. In a simulation in which all the primordial bodies were larger than about 20 km in diameter, at the end all the bodies larger than about 70 km were survivors, but the disruption of smaller ones yielded a tail of fragments sufficient to supply the current comet reservoir.

Varying the collisional parameters that are uncertain for comets (impact strength, strength scaling with size, and f_{KE}) resulted in changes similar to those described above. Weaker bodies showed a greater degree of collisional processing, whereas stronger bodies had less such processing. All cases, though, led to an equilibrium size distribution with the -3.5 power-law exponent at diameters smaller than about 25 km.

In general, our simulations indicate that the population of EKOs larger than about 100 km in diameter is not significantly altered by collisions over the age of the solar system. The size distribution in this range must represent the original accretional population (*9*). Many of these bodies, however, have probably been converted into rubble piles because there is a significant energy gap between the projectile energy needed to shatter the target and that required to disrupt it, that is, to disperse most of the target mass to infinity (*13*, *19*). On the other hand, smaller objects in the EKO population are mostly fragments undergoing a collisional cascade, with a size distribution index close to the -3.5 equilibrium value, provided our assumption of size-independent collisional response parameters is correct. If short-period comets come from the E-K Belt, then 90% of them may not be primitive volatile-rich planetesimals but fragments from larger parent bodies.

As a result of the collisional process, about 10 fragments 1 to 10 km in diameter are currently produced per year in the inner E-K Belt. This estimate refers to the baseline case shown in Fig. 1, with a variability of about a factor of 4, depending on the assumed collisional response parameters. With ejection speeds of 10 to 100 m s^{-1}, which are similar to those inferred for asteroids, these fragments have semimajor axes that differ by about 0.1 to 1.0 AU from those of their parent bodies (Fig. 2). This is sufficient to cause at least a few percent of them (say, 20 such fragments per century) to fall into the resonant escape routes from the E-K Belt (*20*) and to chaotically evolve into the planetary region of the solar system. This is roughly in agreement with the flux required to replenish the short-period comets, which have an estimated population (including inactive nuclei) of 2×10^4 bodies and a mean dynamical lifetime of about 3×10^5 years (*21*). Thus about 0.06 comets per year are needed to maintain this population. If 30% of the E-K Belt fragments that fall into the resonant escape hatches become comets, this is adequate to maintain the population. Therefore, EKO collisions are a sufficient mechanism to supply the short-period comets, just as collisions in the main asteroid belt can supply near-Earth asteroids and meteorites.

The result that most short-period comets are collisional fragments means that these bodies may have experienced some type of structural alteration in the interior of their parent bodies. At a minimum, there would be a modest compacting effect, due to the gravitational self-compression within a parent body's interior. This could explain why not all comets split when they experience thermal or tidal stresses close to the sun or Jupiter. Additional observations that could be explained by a collisional processing of short-period comets are that (i) their irregular triaxial shapes resemble those of fragments produced in breakup events (*22*) and (ii) the variety of colors observed among Centaur and E-K Belt objects can be interpreted as a result of a varying degree of collisional alteration or resurfacing (or both) (*23*). Thus, modeling results and astronomical observations point to collisions as a major process affecting the physical nature of E-K Belt objects and their progeny, the short-period comets.

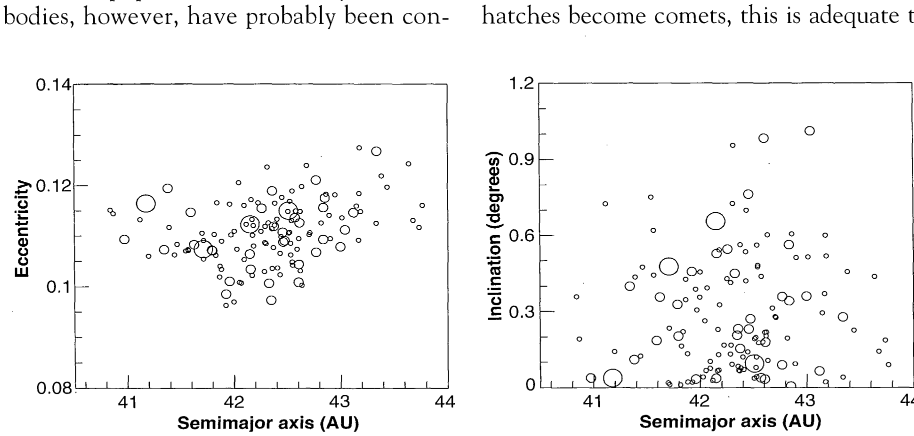

Fig. 2. The distribution of orbital elements for a simulated E-K Belt "family"; that is, for the fragments resulting in our model from a collisional breakup event involving two bodies of 100 and 55 km in diameter, initially orbiting at $a = 42.5$ AU, $e = 0.1$, and $i = 0$. We assumed that a fraction 0.2 of the initial kinetic energy in the center-of-mass reference frame is partitioned into the kinetic energy of the ejected fragments. The larger open circles represent fragments 15 to 40 km in diameter, and the intermediate and smaller ones represent fragments 8 to 15 and 3 to 8 km in diameter, respectively. Note the relatively large spread along the *a* axis, which may result in a significant fraction of the fragments "falling" into chaotic zones associated with resonances.

REFERENCES AND NOTES

1. J. H. Oort, *Bull. Astron. Inst. Neth.* **11**, 91 (1950); K. E. Edgeworth, *Mon. Not. R. Astron. Soc.* **109**, 600 (1949); G. P. Kuiper, in *Astrophysics: A Topical Symposium*, J. A. Hynek, Ed. (McGraw-Hill, New York, 1951), pp. 357–424.
2. M. J. Duncan *et al.*, *Astrophys. J. Lett.* **328**, L69 (1988); T. Quinn *et al.*, *Astrophys. J.* **355**, 667 (1990).
3. V. S. Safronov, *Evolution of the Protoplanetary Cloud and Formation of the Earth and the Planets* (Nauka, Moscow, 1969); J. A. Fernandez, *Mon. Not. R. Astron. Soc.* **192**, 481 (1980).
4. H. Rickman, in *Asteroids Comets Meteors 1993*, A. Milani *et al.*; Eds. (Kluwer, Dordrecht, Netherlands, 1994), pp. 297–312; D. G. Schleicher, *ibid.*, pp. 415–428; S. J. Weidenschilling, *Nature* **368**, 721 (1994).
5. D. Jewitt and J. X. Luu, *Nature* **362**, 730 (1993); *Astron. J.* **109**, 1867 (1995). Updated lists of these objects and their preliminary orbits can be obtained from the Minor Planet Center, which we thank for providing us with these data.
6. Both analytical theories and numerical integrations indicate that EKO eccentricities and sines of the inclination as high as 0.2 would result in long-term chaotic behavior for most bodies in nonresonant orbits [Z. Knežević, A. Milani, P. Farinella, Ch. Froeschlé, C. Froeschlé, *Icarus* **93**, 316 (1991); A. Morbidelli, F. Thomas, M. Moons, *ibid.* **118**, 322 (1996); M. J. Duncan, H. F. Levison, S. M. Budd, *Astron. J.* **110**, 3073 (1995)]. A significant fraction (≈40%) of known (large) EKOs are apparently trapped in stable resonant orbits, particularly the 2:3 mean motion resonance with Neptune. These bodies can have significant eccentricities (0.2 to 0.3) and inclinations (up to ≈25°); however, it is not clear that a significant percentage of all EKOs larger than 1 km in diameter will be similarly located on resonant orbits. Also, we disregard the possibility that EKOs may collisionally interact with a large population of high-eccentricity or high-inclination bodies with semimajor axes >100 AU and perihelia near 40 AU, as predicted by some models for the formation of the Oort cloud [M. Duncan, T. Quinn, S. Tremaine,

Astron. J. **94**, 1330 (1987)], because there is currently no observational evidence for the existence of such a population.
7. A. L. Cochran *et al.*, *Astrophys. J.* **455**, 342 (1996).
8. M. J. Holman and J. Wisdom, *Astron. J.* **105**, 1987 (1993); M. J. Duncan *et al.*, *ibid.* **110**, 3073 (1995).
9. S. A. Stern, *ibid.* **110**, 856 (1995).
10. P_i is the average collision rate per unit of time and per unit of cross-sectional area of the impacting bodies, multiplied by a factor π [G. W. Wetherill, *J. Geophys. Res.* **72**, 2429 (1967)].
11. P. Farinella and D. R. Davis, *Icarus* **97**, 111 (1992); W. F. Bottke *et al.*, *ibid.* **107**, 255 (1994).
12. D. R. Davis and P. Farinella, *Icarus*, in press. For eccentricities and sines of inclination varying between 0.01 and 0.12, $< P_i >$ and $< V >$ range from 4.21×10^{-21} to 0.62×10^{-21} km^{-2} year^{-1} and from 0.39 to 0.81 km s^{-1}, respectively.
13. D. R. Davis *et al.*, in *Asteroids II*, R. P. Binzel, T. Gehrels, M. S. Matthews, Eds. (Univ. of Arizona Press, Tucson, AZ, 1989), pp. 805–826.
14. E. V. Ryan *et al.*, *Icarus* **94**, 283 (1991).
15. A. Lange and T. J. Ahrens, *Lunar Planet. Sci. Conf.* **XII**, 1667 (1981); S. Kawakami *et al.*, *J. Geophys. Res.* **88**, 5806 (1983); M. J. Cintala *et al.*, *Lunar Planet. Sci. Conf.* **XVI**, 1298 (1985); M. Arakawa *et al.*, *Icarus* **118**, 341 (1996).
16. Initial conditions and model parameters for this case are as follows: The initial population was obtained by joining two power laws for the diameter incremental distribution, with exponents -3.5 for $D < 300$ km and -20 for $D \geq 300$ km, and with 13,000 bodies larger than 300 km. Total initial mass: 3 $M_\oplus$. Orbits: $42 < a < 46$ AU; $< e > = 0.05$; and $< \sin i > = 0.05$ (semimajor axis a, eccentricity e, and inclination i). Density: 1.0 g cm^{-3}. Impact strength: 3.0×10^6 erg cm^{-3}. Strength scaling law: energy scaling (size-independent). Fraction f_{KE} of impact energy partitioned into ejecta kinetic energy: 0.1. Exponent of the mass-velocity distribution of fragments: $-9/4$. Crater mass/projectile energy ratio for cratering impacts: 10^{-8} g erg^{-1}.
17. J. W. Dohnanyi, *J. Geophys. Res.* **74**, 2531 (1969); D. R. Williams and G. W. Wetherill, *Icarus* **107**, 117 (1994).
18. A. L. Cochran *et al.*, *Astrophys. J.* **455**, 342 (1995).
19. P. Farinella *et al.*, *Icarus* **52**, 409 (1982).
20. Several mean motion and secular resonances with Uranus and Neptune are present in the E-K Belt and are associated with chaotic dynamics leading to planet-crossing comet-type orbits [A. Morbidelli *et al.*, *ibid.* **118**, 322 (1996); M. J. Duncan *et al.*, *Astron. J.* **110**, 3073 (1995)].
21. H. F. Levison *et al.*, *Icarus* **108**, 18 (1994).
22. D. Jewitt and K. Meech, *Astrophys. J.* **328**, 974 (1988). For a comparison between shapes of asteroids and fragments from hypervelocity impacts, see V. Catullo *et al.*, *Astron. Astrophys.* **138**, 464 (1984).
23. J. X. Luu and D. C. Jewitt, *Astron. J.* **111**, 499 (1996).
24. P.F. acknowledges financial support from the Italian Space Agency (ASI) and the Italian Ministry for University and Scientific Research (MURST). We are grateful to C. Chapman, H. Levison, F. Marzari, A. Milani, A. Stern, S. J. Weidenschilling, and D. E. Wheeler for useful discussions and comments. This is PSI contribution no. 334.

14 March 1996; accepted 5 July 1996

Penetrative Convection and Zonal Flow on Jupiter

Keke Zhang and Gerald Schubert*

Measurements by the Galileo probe support the possibility that the zonal winds in Jupiter's atmosphere originate from convection that takes place in the deep hydrogen-helium interior. However, according to models based on recent opacity data and the probe's temperature measurements, there may be radiative and nonconvective layers in the outer part of the jovian interior, raising the question of how deep convection could extend to the surface. A theoretical model is presented to demonstrate that, because of predominant rotational effects and spherical geometry, thermal convection in the deep jovian interior can penetrate into any outer nonconvective layer. These penetrative convection rolls interact nonlinearly and efficiently in the model to generate and sustain a mean zonal wind with a larger amplitude than that of the nonaxisymmetric penetrative convective motions, a characteristic of the wind field observed at the cloud level on Jupiter.

During its 57 min of descent into Jupiter's atmosphere, the Galileo probe found that the speed of the zonal flow down to about the 20-bar level was nearly constant with depth (*1*). These results suggest that the zonal jet flows in the atmosphere of Jupiter originate from convection that takes place in the deep H-He interior of the planet (*1*). The alternative view that the zonal winds are driven by the latitudinal gradient of solar heating directly in the atmosphere (thermal winds) and thus do not reflect conditions in the deep interior (*2*) seems less likely because the measured winds do not decay with depth.

One model of the internal structure of Jupiter postulates three major layers: an ice-silicate inner core, a metallic fluid H-He layer, and an outer H_2-He envelope (*3, 4*). In the metallic fluid layer, conduction is considered to be insufficient to carry out all the internal energy because thermal photons are unable to propagate in metallic hydrogen (*5*). Thermal convection probably occurs in this region and generates the magnetic field of Jupiter by dynamo processes (*6*). The H_2-He region is also assumed to be convective (*7*), but the outermost zone, at temperatures around 2000 K or less, may contain radiative and stably stratified layers on the basis of interior models incorporating opacity data on H, He, water, ammonia, and methane (*3, 4*). The temperature lapse rate measured by the Galileo probe suggests that the atmosphere between levels of about 5 and 16 bars may be gravitationally stably stratified (*8*), although this hypothesis cannot exclude the possibility that moist convection may take place in this region (*9*). An essential question relating to the deep origin of Jupiter's zonal flow is then whether the deep thermal convection can penetrate through any outermost nonconvective layer of Jupiter.

Penetrative convection occurs in many situations (*10*) and has been studied in nonrotating plane fluid layers (*10–12*). However, for application to Jupiter, rapid rotation and spherical geometry are necessary, and these have not received much attention in the context of penetrative convection. Nonpenetrative convection with rapid rotation and spherical geometry occurs in columnar structures oriented parallel to the rotation axis (*13, 14*).

Busse (*15, 16*) suggested that a multilayered structure of columnar convection rolls might produce the zonal jets in the jovian atmosphere through nonlinear interactions among the rolls. The viability of this hypothesis has been demonstrated in three-dimensional numerical models (*17, 18*) and laboratory simulations (*19*) of high–Rayleigh number convection in a rapidly rotating Boussinesq fluid shell (*20*). Here we demonstrate that similar processes occur even in the presence of a stably stratified layer, so that Jupiter's zonal jets could have a deep convective origin despite the possible existence of radiative, nonconvective outer layers. We also show how penetrative convection rolls interact nonlinearly and effectively to generate and sustain the zonal flows.

The equation of fluid motion for Jupiter's H-He envelope that rotates with constant angular velocity Ω relative to an inertial frame is

$$\frac{d\mathbf{V}}{dt} + 2\Omega\mathbf{k} \times \mathbf{V} = -\frac{1}{\rho}\nabla p + \mathbf{r}B + \nu\nabla^2\mathbf{V} \qquad (1)$$

where $\mathbf{k}$ is a unit vector parallel to Jupiter's rotation axis, $\mathbf{r}$ is the position vector, $\mathbf{r}B$ denotes the small buoyancy force, ν is the kinematic viscosity, ρ is density, $\mathbf{V}$ is the velocity field, and p represents the departure of the pressure from an adiabat. Compressibility and the possible effects of the

K. Zhang, Institute of Geophysics and Planetary Physics, University of California, Los Angeles, CA 90095, USA, and Department of Mathematics, University of Exeter, Exeter, EX4 4QJ, UK.
G. Schubert, Institute of Geophysics and Planetary Physics and Department of Earth and Space Sciences, University of California, Los Angeles, CA 90095, USA.

*To whom correspondence should be addressed.